COMMUNICATIONS DOI: 10.1002/adsc.202001367 Advanced Synthesis & Catalysis

Electronic Effect-Guided Rational Design of *Candida antarctica* Lipase B for Kinetic Resolution Towards Diarylmethanols

Dan-Yang Li,[a] Yu-Jiao Lou,[a] Jian Xu,[a] Xiao-Yang Chen,[b,*] Xian-Fu Lin,[a] and Qi Wu[a,*]

[a] Department of Chemistry
Zhejiang University
Hangzhou 310027, People's Republic of China
Fax (+86)-571-8795-1895
E-mail: wuqi1000@163.com

[b] College of Biological, Chemical Science and Engineering
Jiaxing University
118 Jiahang Road, Jiaxing 314001, People's Republic of China
E-mail: chenxychem@163.com

Manuscript received: November 3, 2020; Revised manuscript received: January 24, 2021;
Version of record online: Februar 5, 2021

Supporting information for this article is available on the WWW under https://doi.org/10.1002/adsc.202001367

Abstract: Herein, we developed an electronic effect-guided rational design strategy to enhance the enantioselectivity of *Candida antarctica* lipase B (CALB) mutants towards bulky pyridyl(phenyl) methanols. Compared to W104A mutant previously reported with reversed *S*-stereoselectivity toward *sec*-alcohols, three mutants (W104C, W104S and W104T) displayed significant improvement of *S*-enantioselectivity in the kinetic resolution (KR) of various phenyl pyridyl methyl acetates due to the increased electronic effects between pyridyl and polar residues. The electronic effects were also observed when mutating other residues surrounding the stereospecificity pocket of CALB, such as T42A, S47A, A281S or A281C, and can be used to manipulate the stereoselectivity. A series of bulky pyridyl(phenyl) methanols, including *S*-(4-chlorophenyl)(pyridin-2-yl) methanol (*S*-CPMA), the intermediate of bepotastine, were obtained in good yields and *ee* values.

Keywords: Rational design; Electronic effect; Lipase; Diarylmethanols; Kinetic resolution

Enantiomerically enriched diarylmethanols continue to emerge with high frequency in disclosures of structural motifs of pharmaceuticals,[1] such as antihistaminic, analgesic, antiarrhythmic, antidepressive, diuretic, laxative, local-anaesthetic and anticholinergic drugs (Figure 1a). Consequently, the efficient synthesis of structurally diverse diarylmethanols, especially in an enantioselective manner is highly coveted. Their preparation typically involves asymmetric addition of aryl nucleophiles to benzaldehyde,[2] or reduction of diaryl ketones *via* asymmetric transfer hydrogenation (ATH)[3] or *via* other biocatalytic transformation processes.[4]

In comparison with traditional chemical catalysts, biocatalysts have inherent advantages such as environmental compatibility, high enantioselectivity, and mild reaction conditions.[5] Ketoreductases or carbonyl reductases were widely used in asymmetric reductions of carbonyl compounds,[6] including diaryl ketones.[7] Recently, Ni and co-workers developed an alcohol dehydrogenase from *Kluyveromyces polyspora* (*Kp*ADH)-catalysed reduction for the synthesis of diarylmethanols, and both configurations of them were obtained *via* iterative combinatorial mutagenesis.[7a] Sun and Nie engineered ADH from *Thermoanaerobacter brockii* (*Tb*SADH) under the guidance of conformational dynamics for the enantioselective transformation of diaryl ketones.[7c]

Kinetic resolution (KR) catalysed by lipase offers an alternative process to achieve enantioselective diarylmethanols. For example, Bäckvall and co-workers utilized the engineered *Candida antarctica* lipase B (CALB), the most extensively used lipase, to establish the resolution of racemic diarylmethanols without any expensive cofactors.[8] According to the study from Hult and coworkers, the hot spot W104, which located in the bottom of the stereospecificity pocket, limited

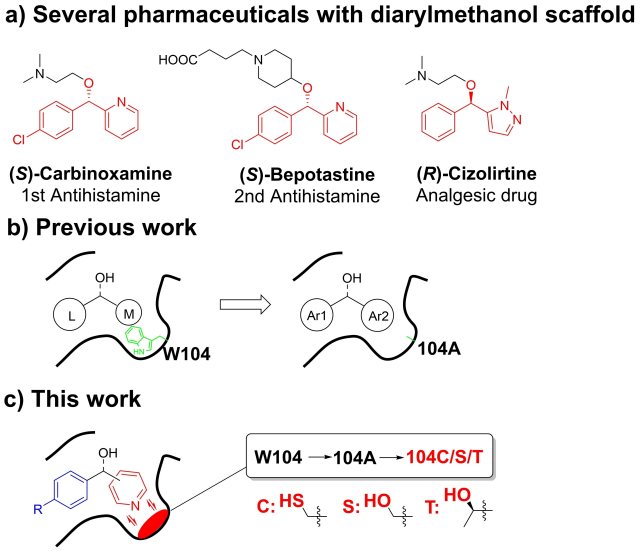

Figure 1. a) Several pharmaceuticals with diarylmethanol scaffold; b) CALB W104A-catalyzed KR of diarylmethanols; c) Electronic effect-guided rational design reported herein for engineered CALB-catalyzed KR of diarylmethanols.

the size of this pocket to fit larger groups than ethyl, and W104A mutant showed wider substrate scopes and reversed enantioselectivity for *sec*-alcohol compared to wide-type (WT).[9] In this significant wok, the authors found that W104A could also catalyze enantioselective transesterification of diarylmethanols. The results showed that the enantioselectivity was mainly dependent on the size difference between two substituents. A larger size-difference led to a higher enantioselectivity. However, the efficient enzymatic KR of diarylmethanols is still challenging because of their high steric hindrance and similarity in size of two aromatic substituents, especially the diarylmethanols substituted by pyridyl and phenyl. Indeed, only 27–74% *ee* values and 2–10 *E* values were observed using 2-, 3- and 4-pyridyl(phenyl)methanols as substrates under the catalysis of W104A (Figure 1b).[8]

Previous results with CALB and other enzymes suggest that apart from steric effects, electronic and solvation effects can also affect the binding of the substrates in enzymes and correspondingly their enantioselectivity.[10] Accordingly, we considered the electronic effects between enzyme and substrates may be more crucial to selectivity than steric attributes in these cases of diarylmethanols with one phenyl and one pyridyl group. Herein, the substrate binding pocket of CALB is rationally engineered to modify the polarity of residues and the cavity volume (Figure 1c), on the basis of the structural cognition of CALB from previous works of our group,[11] thus avoiding the laborious high-throughput screening procedures.[12] We hypothesize the electrostatic attraction and/or hydrogen bonding that involves polar amino acids and substrate's heterocyclic or halogenated moiety might lead to improved enantioselectivity.

The hydrolytic KR of racemic phenyl(pyridin-4-yl) methyl acetate (*rac*-**1a**) was chosen as the model reaction (Scheme 1). This substrate is difficult to be resolved by WT CALB owing to the well-known steric effect of the position W104.[9] When using W104A mutant with the increased significantly volume of binding pocket, a successful KR of **1a** was achieved with good yield and enantioselectivity (50% yield, 91% *ee*, $E = 67$).

W104A mutant was *S*-selective for **1a**, meaning that it can distinguish the two groups with similar size and prefer to bind the more polar pyridyl in the reshaped stereospecificity pocket, probably due to electronic effects between pyridyl and polar residues. In order to further enhance the enantioselectivity of enzymatic KR toward **1a**, we chose three polar amino acids (cysteine (C), serine (S) and threonine (T))[13] with similar size as alanine for the exchange of W104 respectively, to reconstruct a more polar environment of stereospecificity pocket than W104A mutant. W104C mutant displayed a remarkable improvement of *S*-selectivity in comparison with W104A as expected (*ee* and *E* values increased from 91% to 99% and from 67 to >500, respectively, entries 1–2 in Table S4). A similar phenomenon was also observed for W104T. Interestingly, W104S mutant only showed moderate *S*-selectivity for **1a**, perhaps due to the opposite orientation of hydroxyl to pyridyl group.

To probe the molecular mechanisms between target mutants and substrate, *S*-**1a** was docked into W104A and W104C, respectively, then 10 ns molecular dynamics (MD) simulation were performed (Figure 2). As anticipated, the enzyme-*S*-**1a** complex in both mutants matched suitably with the enlarged binding pocked of CALB, which displayed the chief difference from the WT, resulting in high reactivity. In order to further

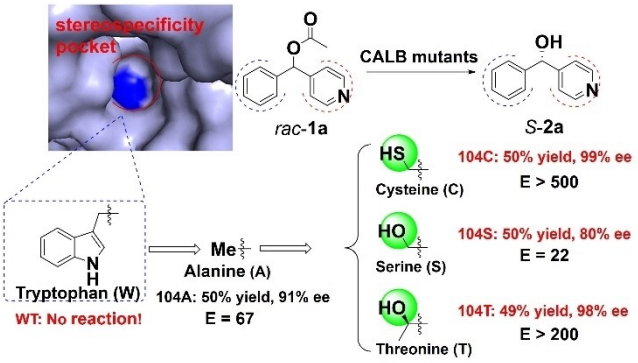

Scheme 1. CALB mutants-catalyzed KR of phenyl(pyridin-4-yl)methyl acetate. Reactions were performed with substrate **1a** (0.01 mmol), acetonitrile (50 μL) and enzymes (~50 μg) in PBS (950 μL, 50 mM, pH = 7.5) at 37 °C.

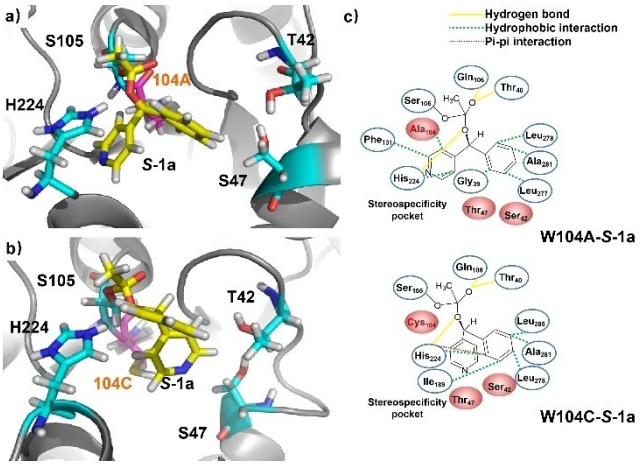

Figure 2. MD optimized structure of W104A (a) and W104C (b) in complex with *S*-**1 a** (yellow). Diagram of interactions between substrate *S*-**1 a** and mutants W104A and W104C (c).

gain insight of the improved selectivity of W104C in comparison with W104A, we focused on the distribution of interactions between *S*-**1 a** and amino acids surrounding the surface of binding pockets (Figure 2c). In W104C, the stereospecificity pocket (C104, S42, T47) focused on maintaining a relatively polar environment with the pyridine group of *S*-**1 a**. In mutant W104A, the polar interaction was weakened, resulting in a reduced enantioselectivity. Nevertheless, compared with W104C, more interactions could be formed in W104A (Figure 2c), which favored a stronger affinity and a lower K_m toward the substrate (Table S2). Although the k_{cat}/K_m of 104C displayed relative decrease compared with 104A, the absolute value was still at a high level revealing high hydrolytic activity.

Inspired by the positive results, phenyl(pyridin-3-yl)methyl acetate (*rac*-**1 b**) and phenyl(pyridin-2-yl) methyl acetate (*rac*-**1 c**) were also tested (Figure 3). All the mutants showed *S*-selectivity toward these two substrates, indicating that the pyridyl groups of *rac*-**1 b** and *rac*-**1 c** bind in the stereospecificity pocket, similarly as **1 a**. Interestingly, enhanced selectivity was obtained by reconstructing the stereospecificity pocket with polar residues in all cases. The best mutant for **1 b** was W104S, which exhibited a decreased selectivity in the KR of **1 a**. For **1 c**, W104C, W104S and W104T gave similar enantioselectivities, indicating a synergistic effect of polar residues and pyridyl group. An acceptable selectivity with W104C was obtained ($E=$ 44, 39% yield, 92% *ee*, entry 21 in Table S4), compared with nonpolar W104A ($E=14$, 40% yield, 78% *ee*, entry 20 in Table S4).

For the electronic effect-guided mutants, the distance between polar OH or SH groups and N atom of pyridyl made a major contribution to the stereoselectivity improvement theoretically.[14] According to

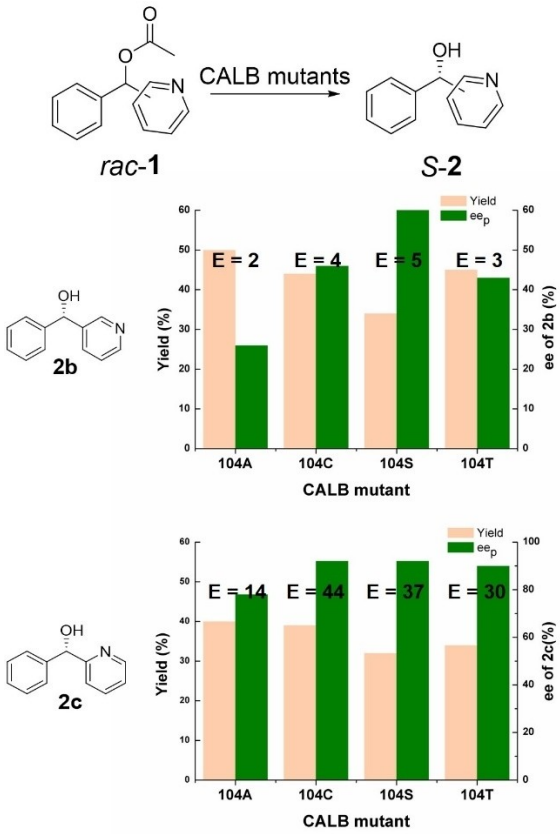

Figure 3. CALB mutants-catalyzed KR of various phenyl pyridyl methyl acetates. Reactions were performed with substrates **1 b** or **1 c** (0.01 mmol), acetonitrile (50 µL) and enzymes (~50 µg) in PBS (950 µL, 50 mM, pH = 7.5) at 37 °C.

the X-ray structure of CALB, the 104 site located in the bottom of the stereospecificity pocket, resulting in a shorter distance and stronger intermolecular force between the 104 polar residues and N atom of pyridin-4-yl (**1 a**) than those of pyridin-3-yl (**1 b**) and pyridin-2-yl (**1 c**). Therefore, the best KR enantioselectivity of **1 a** ($E>200$, entries 2 and 4 in Table S4) catalyzed by CALB mutants was higher than **1 b** ($E=5$, entry 11 in Table S4) and **1 c** ($E=44$, entry 21 in Table S4).

Apart from N atom, halogens also have free electron pairs, which may interact with polar residues. To further evaluate electronic effects on the enantioselectivity of CALB mutants, diarylmethanols substituted with phenyl and halogenated phenyl were studied (Scheme 2). For substrates **1 d**–**1 f**, *R*-enantiomers were the major products under the catalysis of various CALB mutants of W104. The results indicated that the phenyl was the preferential moiety binding into the stereospecificity pocket due to the different steric effect between phenyl and halogenated phenyls. Indeed, the larger size difference between phenyl and halogenated phenyls led to a higher enantioselectivity (**2 d** < **2 e** < **2 f**, Scheme 2). The steric effects were

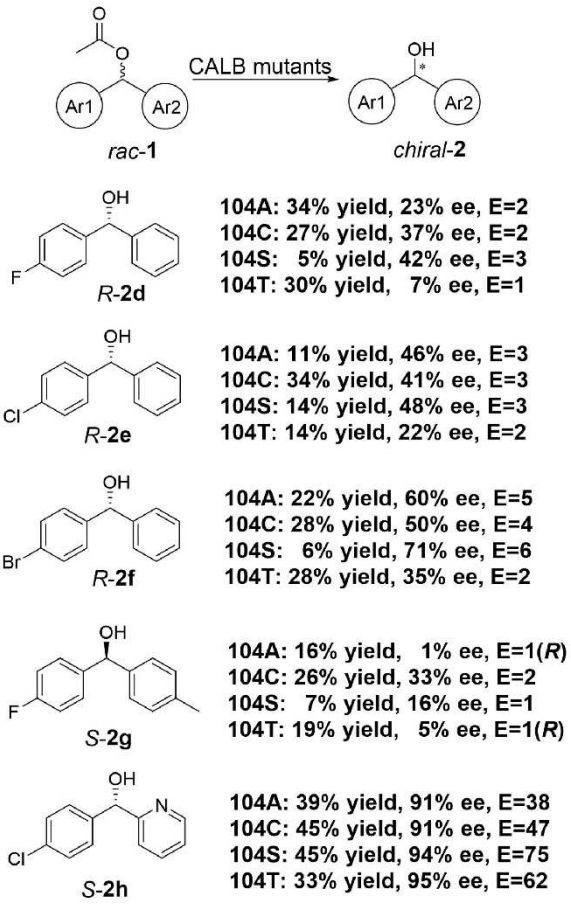

Scheme 2. Enantioselectivity of CALB mutants in the KR towards halogenated diarylmethanols. Reactions were performed with different substrates (0.01 mmol), acetonitrile (50 μL) and enzymes (~50 μg) in PBS (950 μL, 50 mM, pH = 7.5) at 37 °C.

further validated by the enzymatic KR of **1 g**. When the phenyl was replaced by 4-methylphenyl (**1 g**), a larger group than 4-fluorophenyl, 4-fluorophenyl was accommodated into the alcohol-binding pocket and thus reversed (*S*)-selectivity was observed in comparison with **1 d**–**1 f**. For **1 g** with 4-fluorophenyl binding into the active site, electronic effects from 104C or 104S improved the enantioselectivity on different degrees.

One interesting finding is that *S*-(4-chlorophenyl)-(pyridin-2-yl) methanol (*S*-CPMA, *S*-**2 h**), an important precursor for synthesizing the antiallergy drugs bepotastine[15] and carbinoxamine[16] (Figure 1a), was obtained by efficient *S*-selective KR. The electronic effect-guided mutagenesis provided improved variants W104S and W104T for the KR of *rac*-**1 h**. There could be a combination of steric and electronic effects to give an even higher enantioselectivity for **1 h** ($E = 75$, entry 46 in Table S4) than **1 c** ($E = 37$, entry 22 in Table S4) and **1 e** ($E = 3$, entry 34 in Table S4), indicating a cumulative effect. In a preparative scale KR reaction of *rac*-**1 h** (261 mg) under the catalysis of W104S mutant, *S*-**2 h** was obtained in 40% isolated yield (88 mg) with 94% *ee*, meanwhile *R*-**1 h** was recovered in 46% yield (120 mg) and 98% *ee* value (see Supporting information).

To better understand the influence of electronic factors on the enzymatic enantioselectivity, two other polar residues lining the stereospecificity pocket, T42 and S47, were examined. As shown in Figure 4, when introducing T42 A or S47A into the mutant W104A or W104C respectively, the *ee* value decreased remarkably. For example, a double-point mutant 104A/47A hydrolyzed *rac*-**1 b** with negligible enantioselectivity. The introduction of alanine decreased the polarity of stereospecificity pocket, which was crucial for the binding of pyridine ring.

In the KR of *sec*-alcohols containing phenyl and alkyl groups, CALB mutant W104V/A281L/A282K gave the best reversed selectivity compared to WT, according to our previous study,[11c] showing the high affinity between phenyl group and the reshaped stereospecificity pocket. We then further tested this mutant for the KR of substrate *rac*-**1 b**, and obtained a reversed enantioselectivity (Figure 5, entries 17–19 in Table S4), expectedly. Considering the importance of site 281, an alanine located in the large binding pocket,[17] we performed the hydrolysis of *rac*-**1 b** under the catalysis of mutants W104V/A281S and W104V/A281C, respectively. The *R*-selectivity improved significantly, and a good enantioselectivity was observed with W104V/A281S mutant (Figure 5, $E = 28$, 49% yield, 84% *ee*).

To reveal the root of reversed enantiopreference, molecular simulations of substrates *R*-**1 b** and *S*-**1 b**

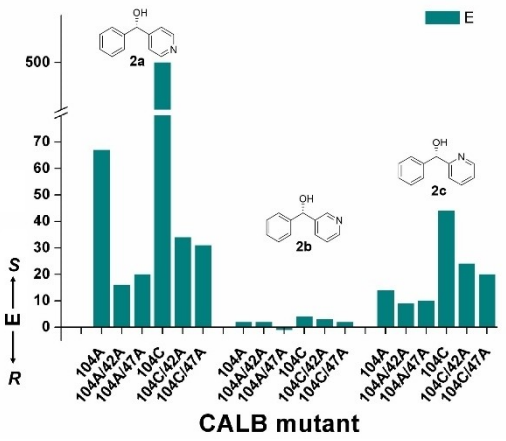

Figure 4. The influence of T42 and S47 to the enzymatic enantioselectivity. Reactions were performed with substrates **1 a**, **1 b** and **1 c** (0.01 mmol, respectively), acetonitrile (50 μL) and enzymes (~50 μg) in PBS (950 μL, 50 mM, pH = 7.5) at 37 °C.

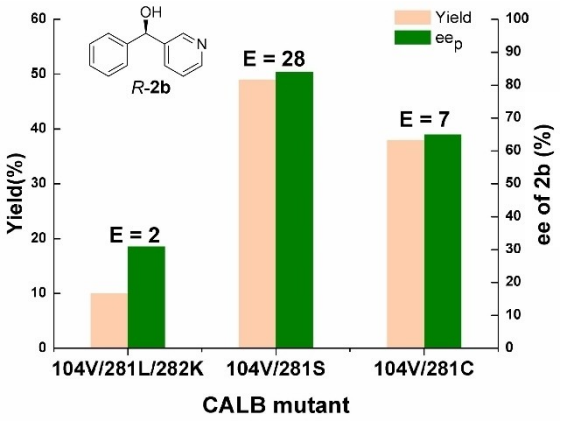

Figure 5. The reversed selectivity of CALB mutants-catalyzed KR of *rac*-**1 b**. Reactions were performed with substrate **1 b** (0.01 mmol), acetonitrile (50 μL) and enzymes (~50 μg) in PBS (950 μL, 50 mM, pH = 7.5) at 37 °C.

were performed for mutant W104V/A281S, respectively (Figure S3). In comparison with 104A, the hydrophobic interaction of 104V was increased significantly (Figure S3, W104V/A281S-*R*-**1 b**), which stabilized the phenyl group. Furthermore, the stronger polarity induced by the S281 offered more stable interactions of pyridine group. It′s worth noting that the hydrogen-bond interaction is observed between S281 and the N atom on pyridine group, to bind the substrate in *R*-Pose, which was also considered as the core effect to convert the selectivity in organic phase in the previous work.[17a] Thus, we considered the above mentioned factors may affect the enantioselectivity reversion, synthetically.

In conclusion, an efficient rational design strategy under the guidance of electronic effect was proposed to enhance the enantioselectivity of the CALB mutants towards bulky pyridyl(phenyl)methanols. The reconstruction of the polar environment at W104 site was performed, and three mutants (W104C/S/T) displayed significant improvement of enantioselectivity for various phenyl pyridyl methyl acetates. In addition, mutating residues T42 or S47 into nonpolar alanine caused a decline of enantioselectivity of these mutants (W104A and W104C). Moreover, the mutants W104V/A281S and W104V/A281C displayed reversed stereoselectivity for the substrate *rac*-**1 b** in comparison with W104C/S/T mutants, because of the reversed binding orientation of pyridyl groups induced by the changed polar environment. These results implied the importance of electronic effects, and even the ability to manipulate the stereoselectivity of enzymes. A series of bulky pyridyl(phenyl) methanols, including *S*-(4-chlorophenyl)-(pyridin-2-yl) methanol (*S*-CPMA), the intermediate of bepotastine, were obtained in good yields and *ee* values. The electronic effect-guided rational design strategy demonstrated herein enables us to engineer various enzymes more conveniently and efficiently to obtain the optically pure products bearing a pyridyl or other heterocycle moieties in further investigation.

Experimental Section

General Procedure of Site-Directed Mutagenesis

A 3-step PCR method was applied to construct all mutants as follows: 94 °C for 5 min, followed by denaturation at 94 °C for 1 min, annealing at 64 °C for 1 min, and elongation at 72 °C for 14 min repeated 30 times, 72 °C for 10 min ended the reaction. The 50 μL PCR mix contained ddH_2O (29 μL), Pfu 10X buffer (5 μL), dNTP (4 μL, 2.5 mM each), forward primers (2 μL, 10 μM each), silent reverse primer (2 μL, 10 μM), WT-CALB plasmid (pETM11-CALB) as DNA template (1 μL, 100 ng/μL) and 1 μL of Pfu polymerase. To ensure elimination of the circular methylated template plasmid, 25 μL of PCR reaction mixture were mixed with 2 μL DpnI (10 U/μL) restriction enzyme at 37 °C for more than 3 h. After digestion, the genes were purified using an Omega Biotek Cycle Pure kit. The PCR product (15 μL) was transformed to 50 μL of *E. coli* Origami2 electrocompetent cells. Transformation mixture was incubated with 1 mL LB medium at 37 °C with shaking at 200 rpm and spread on LB-agar plates containing kanamycin (34 μg/mL) and chloramphenicol (34 μg/mL). All CALB various primers in this work were listed in Table S1 in Supporting Information.

Expression of CALB Mutants

Colonies appeared after cultivation for 12–16 h at 37 °C and were picked into 5.0 mL LB medium containing kanamycin (34 μg/mL) and chloramphenicol (34 μg/mL), and then incubated at 37 °C under shaking at 200 rpm overnight. A fresh 200 mL of TB media was added to 2 mL preculture containing kanamycin (34 μg/mL), chloramphenicol (34 μg/mL) and 1.0 mg/mL L-arabinose as the inducer for expression of chaperone pGro7. The cultures were shaken at 37 °C until the optical density at 600 nm reached 0.6, and then cooled to 4 °C for 1 h. Next, 1.0 mM isopropyl β-thiogalactopyranoside (IPTG) was added into the cultures to induce CALB expression for 48 h at 18 °C. The tubes were centrifuged at 8000 rpm and 4 °C for 5 min, and then the supernatants were discarded. The cell pellet of each tube was resuspended in 50 mM PBS buffer (pH 7.5) and lysed by sonification (15 × 10 sec with 10 sec intervals, at 40% pulse, in a water-ice bath). The cell debris was removed by centrifugation for 25 min at 4 °C. The supernatant was stored at −78 °C.

Hydrolytic Reactions Screening using Substrate 1 a–1 h

50 μL solution of substrate *rac*-**1** (0.25 M in acetonitrile) was added into 5.0 mL EP tubes containing 950 μL crude enzyme. The hydrolytic reaction was performed at 37 °C for the appropriate time. Then the reaction mixture was diluted with MTBE for three times and determined by chiral HPLC. To obtain the isolated yields conveniently, the reaction scale was increased 40 times.

Acknowledgements

This research was funded by National Natural Science Foundation of China (No. 91956128), Zhejiang Provincial Natural Science Foundation (No. LY19B020014), Ph.D. Scientific Research Starting Foundation of Jiaxing University (No. CD70519086) and Scientific Research Starting Foundation of Zhejiang University of Technology (No. 2020105009029).

References

[1] a) F. Schmidt, R. T. Stemmler, J. Rudolph, C. Bolm, *Chem. Soc. Rev.* **2006**, *35*, 454–470; b) J. L. Devalia, C. De Vos, F. Hanotte, E. Baltes, *Allergy* **2001**, *56*, 50–57.

[2] T. Arao, K. Kondo, T. Aoyama, *Tetrahedron Lett.* **2007**, *37*, 4837–4840.

[3] a) E. J. Corey, C. J. Helal, *Angew. Chem. Int. Ed.* **1998**, *37*, 1986–2012; *Angew. Chem.* **1998**, *110*, 2092–2118; b) W. C. Shieh, W. R. Cantrell, J. A. Carlson, *Tetrahedron Lett.* **1995**, *36*, 3797–3800; c) T. Ohkuma, M. Koizumi, H. Ikehira, T. Yokozawa, R. Noyori, *Org. Lett.* **2000**, *2*, 659–662.

[4] a) M. Takemoto, K. Achiwa, *Chem. Pharm. Bull.* **1994**, *42*, 802–805; b) M. D. Truppo, D. Pollard, P. Devine, *Org. Lett.* **2007**, *9*, 335–338.

[5] a) P. N. Devine, R. M. Howard, R. Kumar, M. P. Thompson, M. D. Truppo, N. J. Turner, *Nat. Chem. Rev.* **2018**, *2*, 409–421; b) G. Hughes, J. C. Lewis, *Chem. Rev.* **2018**, *118*, 1–3.

[6] X. Chen, H. L. Zhang, M. A. Maria-Solano, W. D. Liu, J. Li, J. H. Feng, X. T. Liu, S. Osuna, R. T. Guo, Q. Q. Wu, D. M. Zhu, Y. H. Ma, *Nat. Catal.* **2019**, *2*, 931–941.

[7] a) J. Zhou, Y. Wang, G. C. Xu, L. Wu, R. Z. Han, U. Schwaneberg, Y. J. Rao, Y. L. Zhao, J. H. Zhou, Y. Ni, *J. Am. Chem. Soc.* **2018**, *140*, 12645–12654; b) G. C. Xu, Y. Wang, M. H. Tang, J. Y. Zhou, J. Zhao, R. Z. Han, Y. Ni, *ACS Catal.* **2018**, *8*, 8336–8345; c) B. B. Liu, G. Qu, J. K. Li, W. C. Fan, J. A. Ma, Y. Xu, Y. Nie, Z. T. Sun, *Adv. Synth. Catal.* **2019**, *361*, 3182–3190; d) Z. N. Li, Z. X. Wang, Y. H. Wang, X. F. Wu, H. Lu, Z. D. Huang, F. E. Chen, *Adv. Synth. Catal.* **2019**, *361*, 1859–1865; e) B. M. Su, Z. H. Shao, A. P. Li, M. Naeem, J. Lin, L. D. Ye, H. W. Yu, *ACS Catal.* **2020**, *10*, 864–876.

[8] K. Engström, M. Vallin, K. Hult, J. E. Bäckvall, *Tetrahedron* **2012**, *68*, 7613–7618.

[9] A. O. Magnusson, M. Takwa, A. Hamberg, K. Hult, *Angew. Chem. Int. Ed.* **2005**, *44*, 4582–4585; *Angew. Chem.* **2005**, *117*, 4658–4661.

[10] a) J. Bajorath, J. Kraut, Z. Q. Li, D. H. Kitson, A. T. Hagler, *Proc. Natl. Acad. Sci. USA* **1991**, *88*, 6423–6426; b) R. F. Li, H. J. Wijma, L. Song, Y. L. Cui, M. Otzen, Y. E. Tian, J. W. Du, T. Li, D. D. Niu, Y. C. Chen, J. Feng, J. Han, H. Chen, Y. Tao, D. B. Janssen, B. Wu, *Nat. Chem. Biol.* **2018**, *14*, 664–670; c) C. K. Savile, R. J. Kazlauskas, *J. Am. Chem. Soc.* **2005**, *127*, 12228–12229.

[11] a) J. Xu, Y. X. Cen, W. Singh, J. J. Fan, L. Wu, X. F. Lin, J. H. Zhou, M. L. Huang, M. T. Reetz, Q. Wu, *J. Am. Chem. Soc.* **2019**, *141*, 7934–7945; b) Y. Cen, W. Singh, M. Arkin, T. S. Moody, M. Huang, J. Zhou, Q. Wu, M. T. Reetz, *Nat. Commun.* **2019**, *10*, 3198; c) Y. X. Cen, D. Y. Li, J. Xu, Q. S. Wu, Q. Wu, X. F. Lin, *Adv. Synth. Catal.* **2019**, *361*, 126–134; d) B. Xia, J. Xu, Z. Xiang, Y. Cen, Y. Hu, X. Lin, Q. Wu, *ACS Catal.* **2017**, *7*, 4542–4549.

[12] U. T. Bornscheuer, M. Pohl, *Curr. Opin. Chem. Biol.* **2001**, *5*, 137–143.

[13] J. Kyte, R. F. J. Doolittle, *Mol. Biol.* **1982**, *157*, 105–132.

[14] X. Meng, L. Guo, G. Xu, J. P. Wu, L. R. Yang, *J. Mol. Catal. B* **2014**, *109*, 109–115.

[15] A. P. Roszkowski, W. M. Govier, *Pharmacologist* **1959**, *1*, 60–78.

[16] V. Barouh, H. Dall, D. Patel, G. Hite, *J. Med. Chem.* **1971**, *14*, 834–836.

[17] a) B. Yang, R. Lihammar, J. E. Bäckvall, *Chem. Eur. J.* **2014**, *20*, 13517–13521; b) J. Nyhlén, B. Martín-Matute, A. G. Sandström, M. Bocola, J. E. Bäckvall, *ChemBioChem* **2008**, *9*, 1968–1974.

